ISSN 1996-3343

Asian Journal of Applied Sciences

http://knowledgiascientific.com

Knowledgia SCIENTIFIC
A Place to Publish Outstanding Research

Asian Journal of Applied Sciences 5 (6): 404-413, 2012
ISSN 1996-3343 / DOI: 10.3923/ajaps.2012.404.413

The Development of Real 3D Human Digital Model for Design

Y.U. Chi-Yuang and Ming-Hui Liang
Department of Industrial Engineering and Engineering Management, National Tsing Hua University, 101 sec. 2, Kuang Fu Road, Hsinchu, 300, Taiwan

Corresponding Author: Y.U. Chi-Yuang, Department of Industrial Engineering and Engineering Management, National Tsing Hua University, 101 sec. 2, Kuang Fu Road, Hsinchu, 300, Taiwan

ABSTRACT

The objective of this study was to develop a set of real 3D human digital model for design. For each gender, 15 digital models, stratified on 5 heights and 3 weights, of different body sizes were developed based on 3D Taiwanese body bank. The bodybank were scanned in 9 different postures, 1 standing and 8 others, the standing posture was used to construct the digital model and the rest 8 postures were used for evaluation. The skeletal system of the digital model consists of 35 segments and 11 rigid bodies, with 29 joints and 7 end nodes. Each joint is defined in spherical coordinate system with 4 degrees of freedom. The skeleton is organized in 5 paths: 1 torso, 2 upper extremities and 2 lower extremities. Then surface points of segment or rigid body are established as the function of 2 proximal and 2 distal adjacent nodes. Upon the construction of these digital models, they are manipulated to match and superimpose on those 8 different scanned postures. The results show that the maximum mismatch error for each digital model ranges between 25.2 and 37.7 mm, the averaged mismatch error ranges between 4.32 and 10.82 mm. With these maximum and averaged mismatch errors, they are quite promising for product and workplace design application. Later, this set of digital human models has been used to simulate many types of working postures for workplace design.

Key words: 3D digital human model, 3D Taiwanese bodybank, 3D anthropometry

INTRODUCTION

Design dimensions should be measured in functional working posture. The functional posture is defined as the primary posture when a user is using the product or working in the workplace, for instance the driver's seat should be designed when the driver is in driving posture. However, traditionally, product or workplace dimensions are basically determined by 1D measurement, for example, the peeping hole height of a door is determined by standing eye height and table height that is basically referenced to sitting elbow height. However, these 1D dimensions are only good for simple product and workplace dimensions but are usually unsuitable for the dimensions of more complex product and workplace, such as the driver's seat. The driver's seat dimensions, such as design eye position or shifting stick position, should be determined when the driver is assuming driving posture, the so called 'functional posture' (Goossens *et al*., 2000).

In order to take measurements of the functional posture, 2D manikins were greatly used in design in the past, especially in the design of cars and cockpit consoles. 2D manikins also could be used in evaluating human motion (Kim *et al*., 1999). These 2D manikins can only give silhouette profile and motion in sagittal plan and may result in significant error in 3D space. To improve the

shortcoming of 2D manikins, 3D human digital models, such as Jack (EAI) and Ergoman (LAA), were developed. These 3D digital models were reconstructed simply based on 1D dimensions, for example, the upper arm was based on the upper arm length and circumference. And these dummy models could be used in many fields, such as reach and view field test and impact perception evaluations (Lee *et al*., 2002). Although, these 3D human digital models are visually perceived as 3D, their shapes are geometrical and far from real and their motions are robot-like, thus their functional measurements are not accurate. That's why they called "Pseudo 3D digital model" (Roebuck, 1993).

Now-a-days, by the advance of 3D anthropometry scanners, we can obtain a large amount of precise shape of human body in an easy fashion (NASA, 1978; Seong *et al*., 2005). In order to strengthen the shape fidelity and functional measurement accuracy of 3D human digital model, it is attempted to develop a set of 3D digital model based on ever-established 3D Taiwanese bodybank for the design and evaluation of product and workplaces (Yu *et al*., 2003).

MATERIALS AND METHODS

The 3D Taiwanese bodybank is used for the development of 3D digital models. The bodybank were stratified into 15 strata. For each stratum, a representative subject was selected as the based model for 3D human digital model. In all, a set of 15 digital models were developed for each gender.

The digital model was constructed first by matching a stick-skeleton into the base model. The stick-skeleton was a simplified multi-linkage structure resembling our skeletal system. Each link is a representation of a segment and is defined by its proximal and distal nodes.

Secondly, the surface point coordinates of each segment was established as a function of its two nodes and two nearby nodes, so that if the stick-skeleton was moved, the stick-skeleton would brought about the movement of all surface points of that segment.

Finally, the digital models were manipulated to match real scanned data to evaluate the goodness of fit.

The base model: The 3D bodybank, consists of 270 subjects, 135 males and 135 females which were drawn from Taiwanese worker's population, aged between 18 and 64. The distribution was stratified on 5 stature heights and 3 body weights (specified in BMI; body mass index) as listed in Table 1 (Department of Health, 2002). The male has an average height of 167.1±6.26 cm and BMI of 25.9±4.75 and the female has an average height 155.4±5.22 cm and BMI of 25.3±4.62. BMI was used instead of weight because it could be more representative than weight (Bahram and Shafizadeh, 2006; Gholamreza and Mohsen, 2007; Veghari and Golalipour, 2007; Hassan *et al*., 2008; Abu-Samak *et al*., 2008; Nemati *et al*., 2008; Kanaani *et al*., 2010; Hassanzadeh *et al*., 2011). The analyses of variances indicated that the Taiwanese 3D bodybank was not significantly differed from the previous survey (Yu *et al*., 2008).

The 3D bodybank was measured by ITRI Gemini 3D body scanner and a high resolution hand-foot scanner as illustrated in Fig. 1 (Chang *et al*., 2005). The precision and accuracy is within 1.0 mm (Yu *et al*., 2008, 2010). Each subject was measured in 9 postures: 1 standing posture and 8 different postures shown as Fig. 2. The standing posture was used as the base model for the construction of digital models and the rest 8 postures were used for evaluation purpose.

For each stratum, a representative subject was selected as the base model, with the criterion that the representative subject had overall height and body weight the most close to 50%. Here, for

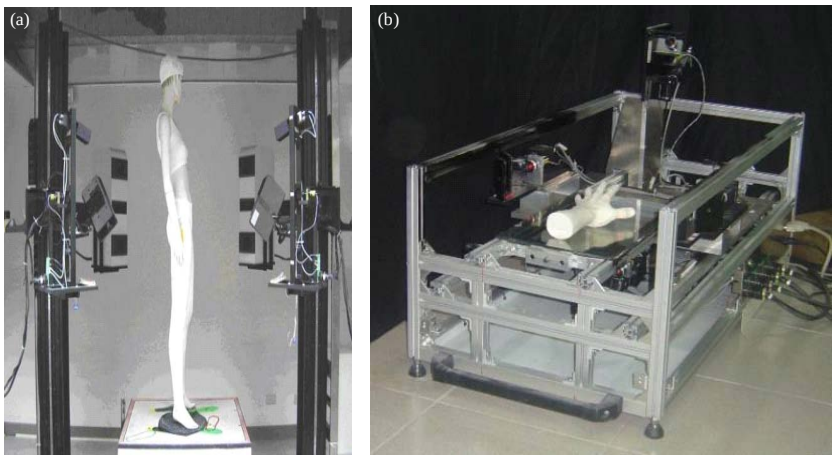

Fig. 1(a-b): Gemini 3D body scanner (a) and a high resolution hand-foot scanner, (b) (Chang *et al*., 2005)

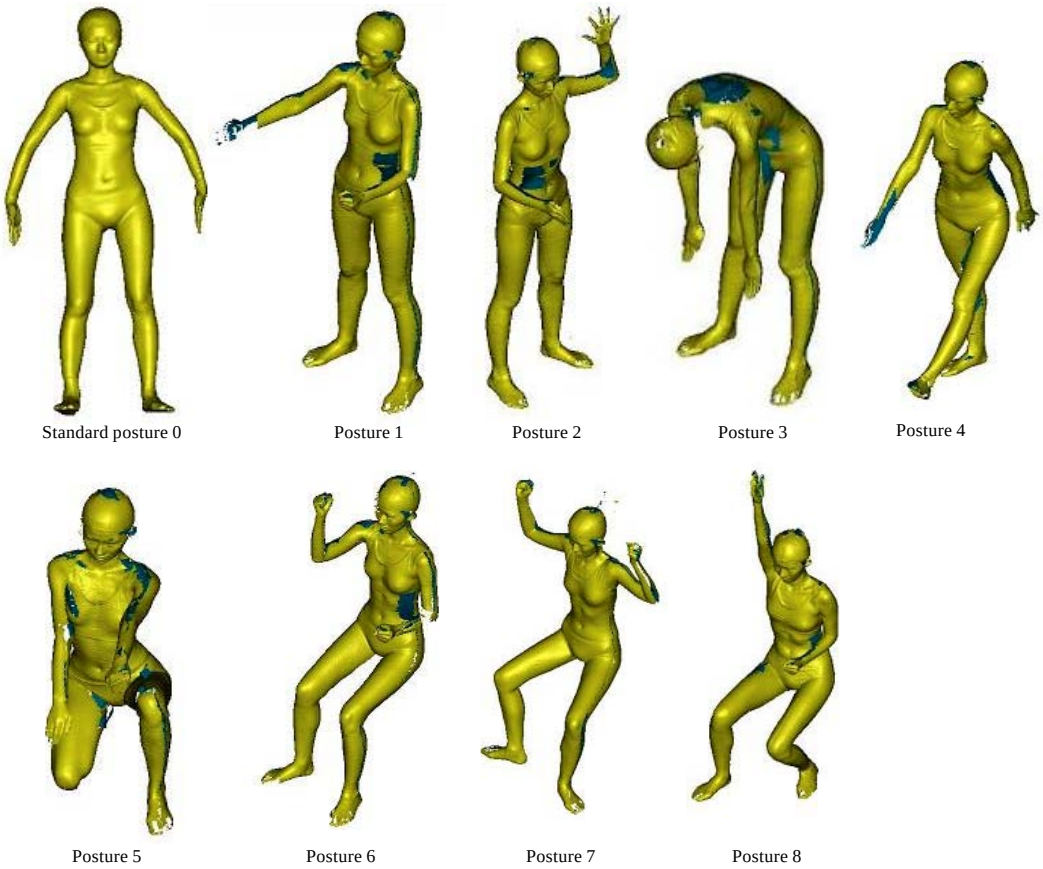

Fig. 2: Nine postures scanned of subject

Table 1: The anthropometric distribution of the 3D bodybank is stratified on 5 stature heights and 3 body weights (BMI) of the male, and the female

Stature height (cm)		Fat (BMI>27)			Medium (18.5<BMI<27)			Slim (BMI<18.5)		
Size	Definition	N	Avg. height (SD)	Avg. BMI (SD)	N	Avg. height (SD)	Avg. BMI (SD)	N	Avg. height (SD)	Avg. BMI (SD)
Male										
XS	<158.1	3	156.8 (0.8)	27.6 (0.36)	4	157.3 (0.8)	22.2 (0.84)	3	153.5 (4.2)	17.8 (0.81)
S	158.1~164.0	10	162.0 (1.4)	28.1 (1.13)	12	161.0 (1.3)	22.1 (0.46)	10	161.5 (2.2)	17.1 (0.69)
M	164.0~169.9	15	168.4 (1.7)	28.3 (2.35)	21	166.5 (2.1)	23.2 (0.93)	15	167.5 (1.2)	17.9 (1.50)
L	169.9~175.8	10	171.3 (1.0)	27.8 (0.20)	12	172.5 (2.3)	24.2 (0.78)	10	171.6 (1.4)	18.2 (1.16)
XL	>175.8	3	179.2 (2.3)	28.3 (0.04)	4	179.3 (1.0)	22.3 (1.55)	3	182.5 (3.3)	18.0 (0.13)
Female										
XS	<147.9	3	145.2 (1.3)	29.2 (1.09)	4	145.7 (2.4)	23.4 (2.15)	3	144.8	17.3 (0.52)
S	1479~152.9	10	151.0 (2.1)	27.5 (0.32)	12	151.0 (2.2)	23.1 (2.18)	10	150.9	17.4 (1.49)
M	152.9~157.9	15	155.3 (1.8)	28.9 (1.46)	21	156.5 (0.7)	24.7 (1.41)	15	155.0	16.8 (1.16)
L	157.9~162.8	10	159.8 (2.0)	29.7 (1.02)	12	161.7 (0.6)	22.6 (1.76)	10	160.2	17.2 (0.74)
XL	>162.8	3	165.3 (2.1)	28.5 (2.13)	4	166.4 (2.3)	22.3 (2.99)	3	164.5	17.5 (0.82)

Male; Male sub.-total, N = 135, Height range = 149.0-~185.5 cm, Avg. = 167.1 cm, SD = 6.26 cm, BMI range = 17.3~29.6, Avg. = 25.9, SD = 4.75. Female; female sub.-total N=135, Height range = 143.0-~168.5 cm, Avg. = 155.4 cm, SD = 5.22 cm, BMI range = 17.2~29.4, Avg. = 25.3, SD = 4.62

Fig. 3: One female base models of the M-medium size

simplicity only 1 female model of the M-Medium size are illustrated here (Fig. 3). It is noted that the base models has no holes on them, they had been carefully hole-filling by template-matching technique (Wu, 2005).

The matching of stick-skeleton into the base model: The stick-skeleton consists of a total of 35 links (segments) which are organized in multi-linkage system with 29 nodes, 7 vertex (end nodes) and in addition 11 rigid bodies, shown as Fig. 4a. The rigid bodies are the segments which are not deformed during body movement, for example, the head and the pelvis.

Like human skeleton, the stick-skeleton is organized in 5 paths: one axial path attached with 2 leg paths and 2 arm paths (Fig. 4b). The axial path originates at pelvis, progresses upward and ends at the cortex of the head. The pelvis is designated as mother node, because it is both the base of the axial and near the mass center of the body. The leg path also originates at pelvis, progresses downward to the foot. The arm path originates at T1 node of the axial path and progresses downward to the hand.

This multi-linkage system is defined in spherical coordinate system. The spherical coordinate system consists of 4 variables (L, θ, ψ, α): L designated as link-length, θ as the including angle between the projection of the link with X-axis, ψ the azimuth angle of the link (to XY plan) and α the rotation angle between the distal and the proximal coordinates (as axial rotation of the link). Then the stick-skeleton was superimposed on the base model and fine tuned by dragging its nodes to register with corresponding rotation center of the base model (Fig. 5). First, several key joint

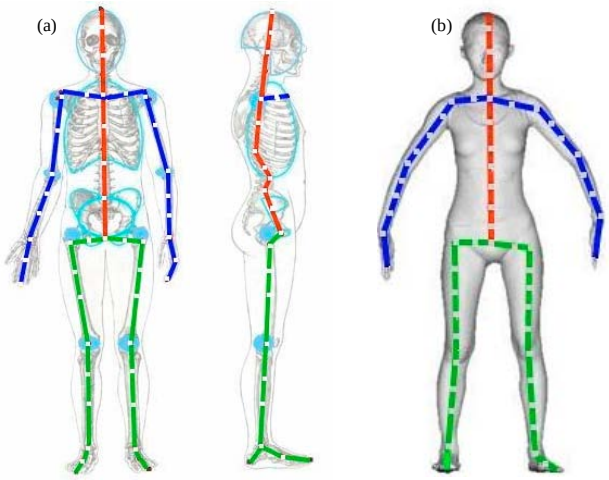

Fig. 4(a-b): (a) The stick skeletal system of digital model and (b) The matched model

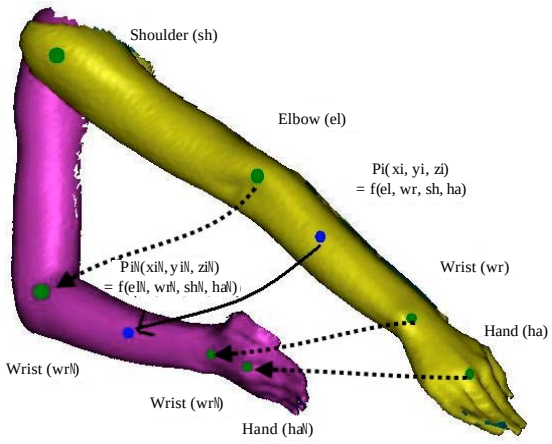

Fig. 5: The surface points in a segment are assigned as the function of the 2 nodes (elbow and wrist) of its correspondent link and/or two other nearby nodes (shoulder and hand)

rotation centers of the base model, such as pelvis, shoulder, elbow, wrist, hip, knee and ankle joints were visually identified on monitor. These joints serve as control points for scaling the stick-skeleton.

The surface points as a function of the stick-skeleton: Next, the relationship between the surface points of the base model and the stick-skeleton was established. The 3D coordinates of each surface point in a segment are assigned as the function of the 2 nodes of its correspondent link and/or two other near by nodes. For example, the 3D coordinates of any surface point Pi on the lower arm are related to the coordinates of the elbow node and wrist node of the lower arm link and in addition to the shoulder node (proximal to elbow node) and the hand node (distal to the wrist node) (Fig. 5). The purpose of these two nearby nodes are used to secure the deformation of surface in the joint region is as smooth and real as possible. Therefore, when the lower arm link was moved in space would bring about the movement of the surface points of the lower arm segment.

Evaluation: Upon the completion of the digital model, the goodness of these digital models was evaluated. The digital model was manipulated into the postures to match the other 8 scanned postures as illustrated in Fig. 2. The manipulated posture was then superimposed onto the scanned postures. The mean and maximal of mismatching error between the two was computed for each posture.

The results of mean and maximal mismatching errors of the 8 postures of the M-Medium male and female were tabulated first and the summary statistics of the minimum, mean and maximum were also calculated. Then likewise, the summary statistics of the 15 males and 15 females were tabulated individually and the overall statistics were also calculated.

RESULTS

The superimposed figures of the digital models and the scan data of the female are presented in Fig. 6. The digital models are colored with purple, while the scan data gold. The purple areas mean that the surface of the digital models are systematically protruded out of the scan data, while the gold areas, on the other hand, are sunk below the scan data. The areas randomly dotted with both colors are perfect match areas.

The results of mean and maximal mismatching error of the 8 postures of the M-Medium male and female are tabulated in the left half of Table 2 and the summary statistics in the right half. For

Table 2: The least square mismatching error (mm) between the digital models and the scanned data of the other 8 postures of male and female

	8 Postures								Summary statistics		
Posture	1	2	3	4	5	6	7	8	Min.	Max.	Mean
Male											
Mean	4.53±2.56	3.02±2.57	4.62±2.60	6.13±2.68	2.25±1.72	8.99±2.63	9.55±3.61	14.86±4.67	2.25±1.72	14.86±4.67	6.74±3.19
Max.	17.93	16.54	18.04	20.44	25.24	23.73	23.07	29.75	16.54	29.75	21.84±4.46
Female											
Mean	5.08±2.69	3.49±2.60	5.04±2.65	5.82±2.76	8.86±2.75	7.58±3.72	9.59±2.76	14.90±3.67	3.49±2.60	14.90±3.67	7.54±2.92
Max.	19.21	17.76	18.56	19.79	22.74	21.09	24.45	28.46	17.76	28.46	21.51±3.58

the male, the average mismatching errors range between 2.25 and 14.86 mm (mean 6.74 mm), the maximal mismatching errors range between 16.54 and 29.75 mm (mean 21.84 mm). For the female, the average mismatching errors range between 3.49 and 14.90 mm (mean 7.54 mm), the maximal mismatching errors range between 17.76 and 28.46 mm (mean 21.51 mm).

Like Table 2, the summary and overall statistics of the 15 male digital models are summarized in Table 3 and the females in Table 4. For the males, the overall mean mismatching errors range between 4.32 and 8.61 mm (mean 6.40 mm), while the maximum mismatching errors range between 25.2 to 33.1 mm (mean 28.72 mm). For the female, the overall mean mismatching errors range between 6.74 and 10.82 mm (mean 7.54 mm), while the maximum errors range between 26.3 to 37.7 mm (mean 30.6 mm).

As a summary to these tables, the results of these 15 male and 15 female digital models seem to be promising in general application, in fact, these 8 scanned postures are extreme postures with maximal torso flexion, arm reach and leg squatting.

Table 3: The mean and maximum mismatching errors (mm) of 15 male digital models

		Body wight (BMI)					
Stature height (cm)		Fat		Medium		Slim	
Size	Definition	Mean ME (SD)	Max. ME	Mean ME (SD)	Max. ME	Mean ME (SD)	Max. ME
Summary statistics of 15 male digital models							
XS	<158.1	6.41 (3.98)	31.3	5.83 (4.21)	28.2	5.13 (3.01)	27.9
S	158.1~164.0	6.13 (4.59)	25.2	5.56 (3.80)	30.3	5.52 (3.23)	26.4
M	164.0~169.9	5.28 (3.09)	28.7	6.74 (4.19)	29.75	8.24 (3.98)	28.1
L	169.9~175.8	8.61 (3.46)	27.7	4.32 (3.87)	33.1	7.78 (4.42)	26.5
XL	>175.8	7.82 (3.58)	25.7	5.89 (3.53)	31.6	6.67 (3.18)	30.3
		Min.		Mean		Max.	
Overall statistics of 15 male digital models							
Mean ME (SD)		4.32 (3.87)		6.40 (4.25)		8.61 (3.46)	
Max. ME		25.2		28.72		33.1	

ME: Mismatching error, Max.: Maximum, Min.: Minimum, SD: Standard deviation

Table 4: The mean and maximum mismatching error (mm) of 15 female digital models

		Body wight (BMI)					
Stature height (cm)		Fat		Medium		Slim	
Size	Definition	Mean ME (SD)	Max. ME	Mean ME (SD)	Max. ME	Mean ME (SD)	Max. ME
Summary statistics of 15 female digital models							
XS	<158.1	6.74 (3.56)	32.3	7.43 (3.78)	28.9	7.30 (3.01)	27.6
S	158.1~164.0	9.10 (3.45)	26.3	9.60 (3.80)	30.8	8.50 (3.83)	26.7
M	164.0~169.9	9.83 (3.23)	29.7	7.54 (3.62)	28.46	8.02 (3.98)	28.6
L	169.9~175.8	9.64 (3.89)	37.7	10.3 (3.87)	35.1	9.18 (3.42)	29.5
XL	>175.8	10.82 (4.58)	28.7	7.90 (3.53)	32.7	8.71 (3.18)	35.3
		Min.		Mean		Max.	
Overall statistics of 15 female digital models							
Mean ME (SD)		6.74 (3.56)		7.54 (4.20)		10.82 (4.58)	
Max. ME		26.3		30.6		37.7	

ME: Mismatching error, Max.: Maximum, Min.: Minimum, SD: Standard deviation

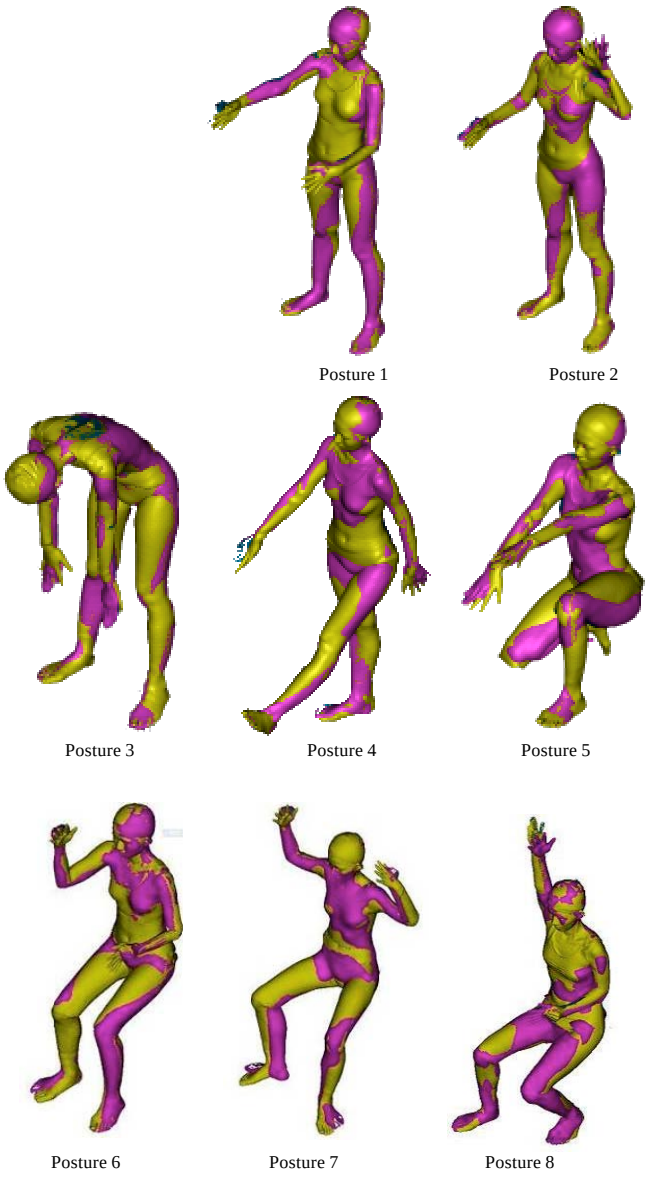

Fig. 6: The superimposed figures of the digital models and the scan data of the female

DISCUSSION

This study is an initial attempt to develop a more anatomically realistic and motion correct digital human model. The base human model used in this study has great body form fidelity, as shown in Fig. 4. The stick-skeleton was designed with enough links (35) for simulating complex joint motion. From results of the supposition figures and mismatch error analyses presented in the results section, these digital models could be thought of much better than Pseudo 3D digital model in terms of realistic body shape and functional posture accuracy, it should be highlighted that the maximal mismatch error for these digital model is less than 37.7 and in average the mismatch error is 6.40 and 7.54 mm.

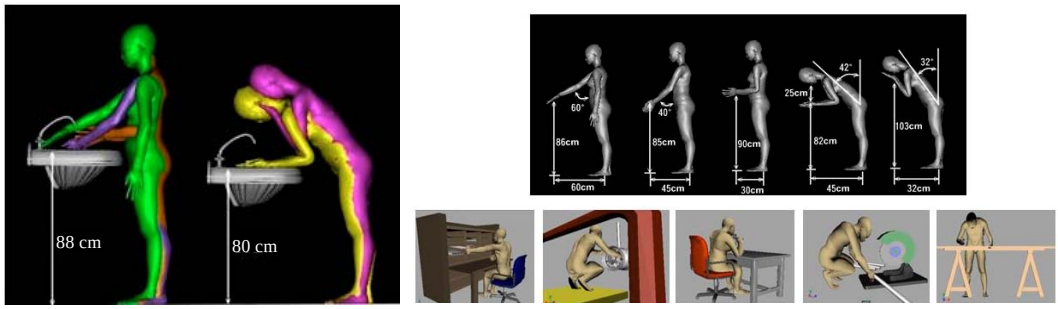

Fig. 7: Digital human models as design guideline for the design and innovation of workplaces

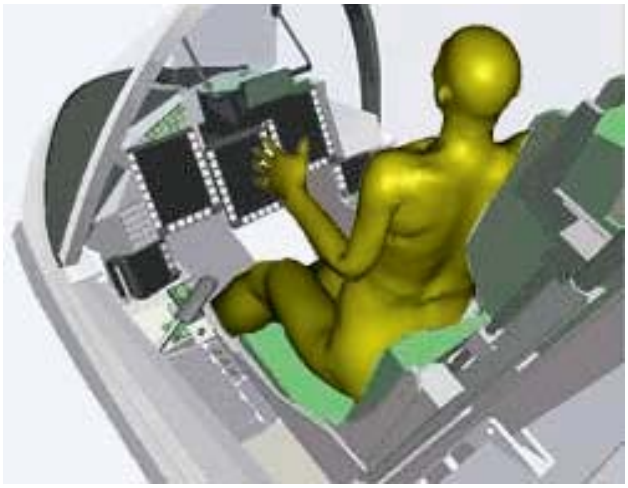

Fig. 8: The incorporation of digital human models with CAD/CAE

This would be quite promising in product and workplace design application. These models could address safety concerns on the digital mock-ups in computer, long before physical prototypes are constructed. For example, the contour of the seat-pan and backrest can be designed with great fit. The hand reach envelope can be estimated with great accuracy. These digital human models could also be applied in evaluating human postures as in virtual simulation.

To date, this set of digital human models has been used to simulate many types of working postures for workplace design (Azadeh *et al*., 2007). A booklet entitled "A collection of workplace design" which consists of 100 representative workplaces, was compiled for use as design guideline for the design and innovation of workplaces (Chang *et al*., 2005) (Fig. 7). It is postulated that these digital human models can be further incorporated with Computer-aided Design (CAD) and Computer-aided Engineering (CAE) in the future (Fig. 8).

REFERENCES

Abu-Samak, M., R. Khuzaie, M. Abu-Hasheesh, M. Jaradeh and M. Fawzi, 2008. Relationship of vitamin B12 deficiency with overweight in male Jordanian youth. J. Applied Sci., 8: 3060-3063.

Azadeh, A., I. Mohammad Fam and M.M. Garakani, 2007. A total ergonomic design approach to enhance the productivity in a complicated control system. Inform. Technol. J., 6: 1036-1042.

Bahram, A. and M. Shafizadeh, 2006. A comparative and correlational study of the body-image in active and inactive adults and with body composition and somatotype. J. Applied Sci., 6: 2456-2460.

Chang, C.P., C.Y. Chen and C.Y. Yu, 2005. Renewing of existing indigenous anthropometric database and its application on the facility measurement of workplace (III). Report No. IOSH94-H314, Institute of Occupational Safety and Health, ROC (Taiwan).

Department of Health, 2002. The definition of obesity and dealing principles of national in Taiwan. http://www.doh.gov.tw/CHT2006/DM/DM2_p01.aspx?class_no=25&now_fod_list_no=3942&level_no=2&doc_no=32

Gholamreza, V. and S. Mohsen, 2007. The comparative study of body mass index distribution among preschool children in a 7 years period in North of Iran. J. Applied Sci., 7: 2681-2685.

Goossens, R.H., C.J. Snijders and T. Fransen, 2000. Biomechanical analysis of the dimensions of pilot seats in civil aircraft. Applied Ergonomics, 31: 9-14.

Hassan, N.E., S.A. El-Masry, N.L. Soliman and M.M. EL-Batran, 2008. Different techniques for body composition assessment. J. Med. Sci., 8: 15-21.

Hassanzadeh, K., P. Yavari-Kia, H. Soleymanpour, N. Ebrahimpour-Tolouei and H. Alikhah, 2011. Effect of body mass index on severity and prevalence of varicocele. Pak. J. Biol. Sci., 14: 869-875.

Kanaani, J.M., S.B. Mortazavi, A. Khavanin, R. Mirzai, Y. Rasulzadeh and M. Mansurizadeh, 2010. Foot anthropometry of 18-25 years old Iranian male students. Asian J. Scient. Res., 3: 62-69.

Kim, C.H., B.G. Oh and S.H. Kim, 1999. Human motion control using dynamic model human motion control using dynamic model. J. Ergon. Soc. Korea, 18: 141-152.

Lee, S.C., K. Sohn and S.J. Kim, 2002. Development and application of Korean dummy models development and application of korean dummy models. J. Ergonomics Soc. Korea, 21: 13-23.

NASA, 1978. Anthropometry Source Book. Yellow Spring, Ohio, USA., pp: 60-62.

Nemati, A., M. Barak, A N. Baghi, N. Abbasgholizadeh and F. Homapour *et al.*, 2008. Relationships between anthropometrical indices and socio-economic differences for children at 6 years old living in urban areas of ardebil, Iran. J. Applied Sci., 8: 3748-3752.

Roebuck, J.A., 1993. Anthropometric Methods: Designing to Fit the Human Body. Human Factors and Ergonomics Society, Santa Monica, USA., Pages: 199.

Seong, D.H., E.S. Jung and Y.J. Cho, 2005. A methodology for developing a Korean apparel sizing system by body types. J. Ergonomics Soc. Korea, 24: 31-37.

Veghari, G.R. and M.J. Golalipour, 2007. The comparison of nutritional status between Turkman and non-Turkman ethnic groups in North of Iran. J. Applied Sci., 7: 2635-2640.

Wu, Y.C., 2005. Filling holes in 3D scanned body surfaces data using template matching method. Master's Theses, Tsing Hua University, Xinzhu, Taiwan.

Yu, C.Y., C.H. Lin and Y.H. Yang, 2010. Human body surface area database and estimation formula. Burns, 36: 616-629.

Yu, C.Y., Y.H. Lo and W.K. Chiou, 2003. The 3D scanner for measuring body surface area: A simplified calculation in the Chinese adult. Applied Ergon., 34: 273-278.

Yu, C.Y., Y.W. Hsu and C.Y. Chen, 2008. Determination of hand surface area as a percentage of body surface area by 3D anthropometry. Burns, 34: 1183-1189.